Nonlinear Landau-Zener-Stückelberg-Majorana problem with non-Hermitian models

Y. Cao and T. F. Xu*

State Key Laboratory of Metastable Materials Science and Technology and Key Laboratory for Microstructural Material Physics of Hebei Province, School of Science, Yanshan University, Qinhuangdao 066004, People's Republic of China

(Received 21 August 2023; revised 8 December 2023; accepted 8 January 2024; published 30 January 2024)

We study nonlinear Landau-Zener-Stückelberg-Majorana (LZSM) tunneling with a $\mathcal{PT}$-symmetric potential, which can be converted to a non-Hermitian nonlinear two-level model by a two-mode approximation. Then, we construct an equivalent Hermitian model through a transformation, verify that the tunneling probabilities obtained by the two models are consistent, and comprehensively analyze the effect of the gain-dissipation term on tunneling. In addition, due to the gain-dissipation properties, the total population density of the non-Hermitian model is no longer a conserved quantity, which will increase or decay to a fixed value as the model evolves. Finally, we prove that the spatial inversion symmetry breaking of the Hamiltonian leads to nonreciprocal tunneling, and the numerical simulation results confirm our analysis. These studies provide alternative ideas to study the nonlinear dynamics of non-Hermitian systems in the future.

DOI: 10.1103/PhysRevA.109.012622

I. INTRODUCTION

As the foundation of modern science, quantum mechanics has provided a theoretical framework for studying the microcosmic world since its birth. In traditional quantum theory, observations are treated as Hermitian operators in Hilbert space with eigenvalues of real numbers, which ensures many properties of conservative systems. In 1998, a class of non-Hermitian Hamiltonian systems following parity-time ($\mathcal{PT}$) symmetry was reported [1], immediately attracting wide attention in the scientific community. This discovery modified the traditional quantum theory and revolutionized quantum theory into a new field. In scientific research, dissipation always exists. Scientists think it is a harmful physical effect, and adopt various methods to compensate for it. However, the $\mathcal{PT}$ system introduces dissipation into the Hamiltonian. Still, it has real eigenvalues, which shows that the system can still maintain the properties of conservative systems. This novel characteristic makes dissipation more meaningful in physical research [2]. This opens up new possibilities for the control of physical systems and has a wide range of applications in many fields, such as plasma physics [3,4], Bose-Einstein condensation (BEC) [5], nonlinear optics [6–8], and so on.

Tunneling is one of the most common phenomena in quantum mechanics. The problem of a system crossing from one side to the other to avoid the crossing of energy levels under an external linear drive is called Landau-Zener-Stückelberg-Majorana (LZSM) tunneling, in honor of the outstanding contributions made by these four scientists [9–12]. The LZSM problem has important applications in various physical systems [13–17]. In particular, Wu *et al.* found that a loop structure will appear in the lowest-energy band with increased nonlinear intensity, which is proved in Ref. [18]. This special band structure leads to the appearance of an unstable superposition state [19]. Based on the equivalent classical Hamiltonian, the physical mechanism is studied, and the adiabatic tunneling phenomenon caused by the loop structure is revealed [20]. These findings further extend the LZSM tunneling problem to nonlinear physics, which is inherent in many fields of physics. The loop structure and adiabatic tunneling lead to various new phenomena, which have triggered a lot of research and discussion in the scientific community, but these studies are limited to Hermitian systems [21–25].

In this paper, we consider the non-Hermitian nonlinear two-level model, which is also mentioned in recent studies [26–28]. This model can be equivalent to a Hermitian Hamiltonian. The research shows a threshold value of the gain-dissipation term. Below and beyond it, the effect of this term on adiabatic tunneling is the opposite. Furthermore, as the linear driving intensity increases, a crossover point exists where gain-dissipation plays a major role in the smaller driving part. The nonlinear intensity significantly affects the position of the crossover point. The paper is structured as follows. In Sec. II, we introduce our non-Hermitian model and its equivalent Hermitian model, prove their tunneling probabilities are consistent, and obtain the specific expressions of the gain-dissipation coefficient threshold and total population density. Then, we detail the case of reverse sweep in Sec. III and conclude in Sec. IV.

II. MODEL

The present work considers a dimensionless generalized Gross-Pitaevskii equation of the following form,

$$i\frac{\partial\psi}{\partial z} = -\frac{1}{2}\frac{\partial^2\psi}{\partial x^2} + V(x)\psi - \beta x\psi + c|\psi|^2\psi, \qquad (1)$$

*tfxu@ysu.edu.cn

with $V(x)$ being a $\mathcal{PT}$-symmetric periodic function. In this paper, we discuss the known potential

$$V(x) = v_0[\cos^2 x + i\omega_0 \sin(2x)], \tag{2}$$

where v_0 is the depth of the potential and ω_0 is the gain-dissipation coefficient. When $\omega_0 \geqslant 0.5$, the lowest two bands degenerate, and the degenerate bands appearing imaginary part, the energy gap disappears [29]. What appears here is no longer the LZSM tunneling phenomenon. Therefore, we only consider the $\omega_0 < 0.5$ part in this paper. βx denotes an external transverse bias. Here, β is the external driving intensity and experimentally controls the sweep rate and direction. c is the Kerr nonlinear coefficient, where $c > 0$ and $c < 0$ indicate repulsive and attractive interactions, respectively. We can convert Eq. (1) to the following form through a gauge transformation,

$$i\frac{\partial\tilde{\psi}}{\partial z} = \frac{1}{2}\left(-i\frac{\partial}{\partial x} + \beta z\right)^2 \tilde{\psi} + V(x)\tilde{\psi} + c|\tilde{\psi}|^2\tilde{\psi}, \tag{3}$$

where $\tilde{\psi} = e^{-i\beta xz}\psi$. Here, we can define a pseudomomentum vector

$$k(z) = k_0 + \alpha z. \tag{4}$$

The value of α is the same as β, but we use a different notation because of the different physical meanings. α is called the sweep rate, and its sign represents the sweep direction. We define $\alpha > 0$ as the forward sweep, $\alpha < 0$ as the reverse sweep, and $\alpha = 0$ as the adiabatic process. Furthermore, k_0 is an arbitrary Bloch vector in the Brillouin zone. If the system's initial state is a Bloch state in the lowest Bloch band, when β is small enough, the system will oscillate in the band, which is called Bloch oscillation. As β increases, the system will tunnel toward the upper band at the Brillouin zone's edge ($k_{\mathrm{BZ}} = 1$). However, tunneling between higher bands requires more energy, making tunneling more difficult. Therefore, when v_0 is sufficiently small, we can consider only two modes as resonant, which are coupled by the Bragg scattering, and ignore the higher mode, i.e.,

$$\psi(x, z) = e^{ik(z)x}[a_0(z) + a_1(z)e^{-i2x}], \tag{5}$$

which is called two-mode approximation [8] and is often used to study tunneling in BEC [30,31]. Here, we can take $k_0 = 1$ so that the minimum band gap occurs at $\alpha z = 0$, i.e., $k(z) = 1 + \alpha z$. a_0 and a_1 represent the amplitudes of the two plane-wave components and satisfy the normalization condition $|a_0|^2 + |a_1|^2 = 1$. Substitute Eq. (5) into Eq. (1) and make the following variable substitutions,

$$\begin{pmatrix} a \\ b \end{pmatrix} = \exp\left[i\left(\frac{1}{2}z + \frac{1}{6}\alpha^2 z^3 + \frac{v_0}{2}z + \frac{3}{2}cz\right)\right]\begin{pmatrix} a_0 \\ a_1 \end{pmatrix}. \tag{6}$$

Then, we will obtain a nonlinear two-level model (NTL),

$$\begin{aligned} i\frac{\partial}{\partial z}\begin{pmatrix} a \\ b \end{pmatrix} &= \begin{pmatrix} \gamma + \frac{c}{2}(|b|^2 - |a|^2) & \frac{v_0}{4} + \frac{v_0\omega_0}{2} \\ \frac{v_0}{4} - \frac{v_0\omega_0}{2} & -\gamma - \frac{c}{2}(|b|^2 - |a|^2) \end{pmatrix}\begin{pmatrix} a \\ b \end{pmatrix} \\ &= H(\gamma)\begin{pmatrix} a \\ b \end{pmatrix}. \end{aligned} \tag{7}$$

Here, we introduce the notation $\gamma = \alpha z$. It can be seen that the Hamiltonian $H(\gamma)$ in Eq. (7) is non-Hermitian and has the same form as Ref. [27] when it is in the linear case. We take a transformation of Eq. (7) to get the following form,

$$i\frac{\partial}{\partial z}\left[\eta^{-1}\begin{pmatrix} a \\ b \end{pmatrix}\right] = \eta^{-1}H\eta\eta^{-1}\begin{pmatrix} a \\ b \end{pmatrix} + i\left(\frac{\partial}{\partial z}\eta^{-1}\right)\begin{pmatrix} a \\ b \end{pmatrix}. \tag{8}$$

If we can find an η matrix without z, we can reduce it to a form similar to Eq. (7), i.e.,

$$i\frac{\partial}{\partial z}\begin{pmatrix} a' \\ b' \end{pmatrix} = H_\eta\begin{pmatrix} a' \\ b' \end{pmatrix}. \tag{9}$$

Here,

$$H_\eta = \eta^{-1}H\eta, \quad \begin{pmatrix} a' \\ b' \end{pmatrix} = \eta^{-1}\begin{pmatrix} a \\ b \end{pmatrix}. \tag{10}$$

Since the linear adiabatic tunneling probability $P_{\mathrm{lin}} = \exp[-\pi\delta^2/(2|\alpha|)]$ is only determined by the band-gap width δ when the sweep rate is fixed, we first calculate the adiabatic energy level $E_{\mathrm{lin}} = \pm\sqrt{(\frac{v_0}{4})^2 - (\frac{v_0\omega_0}{2})^2 + \gamma^2}$ corresponding to Eq. (7) and find its band-gap width, that is, the minimum energy gap difference is $\Delta = \frac{1}{2}v_0\sqrt{1 - 4\omega_0^2}$. Therefore, we can define a Hermitian matrix,

$$H_\eta = \begin{pmatrix} \gamma + \frac{c}{2}(|b|^2 - |a|^2) & \frac{1}{2}\Delta \\ \frac{1}{2}\Delta & -\gamma - \frac{c}{2}(|b|^2 - |a|^2) \end{pmatrix}. \tag{11}$$

This ensures that the LZSM tunneling probability in the linear case of Eq. (9) is consistent with Eq. (7). Fortunately, under such a definition, we can find an η matrix without z in the following form,

$$\eta = \begin{pmatrix} \eta_{11} & 0 \\ 0 & \eta_{22} \end{pmatrix}, \tag{12}$$

where η_{11} and η_{22} are undetermined values. After calculation, we can get

$$\begin{aligned} \eta &= \begin{pmatrix} \sqrt{v_0 + 2v_0\omega_0} & 0 \\ 0 & \sqrt{v_0 - 2v_0\omega_0} \end{pmatrix}, \\ \eta^{-1} &= \begin{pmatrix} (v_0 + 2v_0\omega_0)^{-\frac{1}{2}} & 0 \\ 0 & (v_0 - 2v_0\omega_0)^{-\frac{1}{2}} \end{pmatrix}. \end{aligned} \tag{13}$$

According to the above series of derivations and definitions, we can rewrite Eq. (7) as an equivalent nonlinear two-level model (ENTL),

$$\begin{aligned} i\frac{\partial}{\partial z}\begin{pmatrix} a' \\ b' \end{pmatrix} &= \begin{pmatrix} L & \frac{1}{4}v_0\sqrt{1 - 4\omega_0^2} \\ \frac{1}{4}v_0\sqrt{1 - 4\omega_0^2} & -L \end{pmatrix} \\ &= H_\eta\begin{pmatrix} a' \\ b' \end{pmatrix}, \end{aligned} \tag{14}$$

with $L = \gamma + \frac{c}{2}[(v_0 - 2v_0\omega_0)|b'|^2 - (v_0 + 2v_0\omega_0)|a'|^2]$. We call H_η and $\binom{a'}{b'}$ the equivalent Hamiltonian and equivalent component of Eq. (7). To understand the behavior of tunneling probability with parameters, we set the initial state ($\gamma \to -\infty$) of NTL to $(a, b) = (1, 0)$, and then directly evolve Eq. (7) by the Crank-Nicolson method [32] and time splitting method [33] to get $|a|^2$ at $\gamma \to \infty$, which is the tunneling

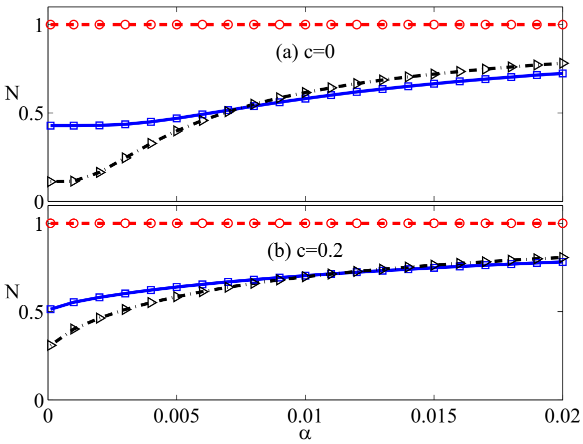

FIG. 1. The final total population density N under forward sweep for $v_0 = 0.2$. Dashed (red), solid (blue), and dashed-dotted (black) lines correspond to NTL simulation results at $\omega_0 = 0$, 0.2, and 0.4, respectively. Red circles, blue squares, and black triangles correspond to $N = \frac{1-2\omega_0}{1+2\omega_0} + \frac{4\omega_0}{1+2\omega_0}P$ at $\omega_0 = 0$, 0.2, and 0.4, respectively. Here, P is the tunneling probability under forward sweep (see Fig. 2).

probability P [13]. Similarly, for our ENTL, the corresponding equivalent initial state is $(a', b') = [(v_0 + 2v_0\omega_0)^{-1/2}, 0]$, in this case $N' = |a'|^2 + |b'|^2 = 1/(v_0 + 2v_0\omega_0)$. Therefore, we can obtain the tunneling probability corresponding to ENTL, $P' = |a'|^2/N' = P$, that is, the tunneling probability obtained by the two models should be consistent. In addition, since NTL is non-Hermitian, its population density N is not conserved. However, ENTL is Hermitian and N' is conserved, so we can obtain $N = |a|^2 + |b|^2 = \frac{1-2\omega_0}{1+2\omega_0} + \frac{4\omega_0}{1+2\omega_0}P$ for NTL at $\gamma \to \infty$ by Eq. (10). Due to dissipation, the total population density N decays to a fixed value, which is associated with ω_0 and α, and this has been similarly concluded in Refs. [30,34] (see Fig. 1).

Next, to verify the validity of the two-mode approximation, we consider the exact solution of the tunneling probability between the lowest two bands of Eq. (1) by using the known LZSM formula $P'_{\rm lin} = \exp(-\pi\Delta_0^2/2\alpha)$, and compare it with the probability simulated by ENTL when $c = 0$. Δ_0 is the minimum energy difference between the lowest two bands without an external transverse bias. For Eq. (1) of $\beta = 0$ and $c = 0$, we are looking for the solution in the following form,

$$\psi(x, z) = \exp(-i\mu_0 z + iKx) \sum_{n=-N}^{N} a_n \exp(i2nx). \qquad (15)$$

Here, the summation term on the right-hand side of the equation is called the plane-wave expansion, also known as the Fourier expansion. μ_0 and K are energy levels and Bloch wave numbers, respectively. We then substitute Eq. (15) into Eq. (1), numerically calculating the band-gap width Δ_0 and get the tunneling probability. In Fig. 2(a) we compare this probability with the one obtained from the two-level model. This result shows that our two-mode approximation is valid, and in fact, Ref. [8] proves that this approximation is true when v_0 is small. In this section, if not specifically emphasized, we research ENTL all under forward sweep.

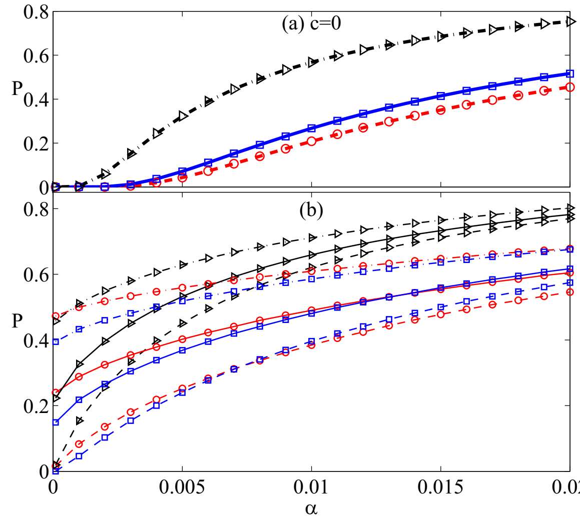

FIG. 2. Tunneling probability P for $v_0 = 0.2$ under forward sweep. (a) Bottom to top corresponds to $\omega_0 = 0$, 0.2, and 0.4, respectively. Circles, squares, and triangles correspond to the numerical simulation results of ENTL. Dashed (red), solid (blue), and dashed-dotted (black) lines represent the exact solutions obtained from the plane-wave expansion and the LZSM formula $P'_{\rm lin}$. (b) Red circles, blue squares, and black triangles correspond to ENTL simulation results at $\omega_0 = 0$, 0.2, and 0.4, respectively. Dashed, solid, and dashed-dotted lines correspond to $c = 0.1$, 0.2, and 0.4, respectively. For instance, a solid line with circles corresponds to $c = 0.2$ and $\omega_0 = 0$.

As can be seen from Fig. 2, with the rise of the external driving intensity, the tunneling probability quickly exceeds the case of $\omega_0 = 0$, and the larger the nonlinear coefficient c and gain-dissipation coefficient ω_0, the closer the intersection point is to the adiabatic case. These phenomena all indicate that the appearance of gain-dissipation makes the system more sensitive to the response of the external drive. Since the nonlinear adiabatic tunneling is closely related to the loop structure of the adiabatic level, we need to consider the behavior of adiabatic levels in ENTL. These levels are obtained by replacing $i\partial/\partial z$ in Eq. (14) with energy μ, i.e., Eq. (14) is reduced to a z-independent version by the component variable method. That is to say, $\mu\binom{a'}{b'} = H_\eta\binom{a'}{b'}$. Then, we find the following quartic equation satisfied by the energy μ,

$$\mu^4 + A\mu^3 + B\mu^2 + C\mu + D = 0, \qquad (16)$$

where

$$\begin{aligned} A &= \frac{c}{1+2\omega_0}, \\ B &= \frac{c^2 - 2c^2\omega_0 + 8c\omega_0\gamma}{4+8\omega_0} - \frac{v_0^2(1-4\omega_0^2)}{16} - \gamma^2, \\ C &= -\frac{cv_0^2(1-2\omega_0)}{16}, \\ D &= -\frac{c^2v_0^2(1-2\omega_0)}{64(1+2\omega_0)}. \end{aligned} \qquad (17)$$

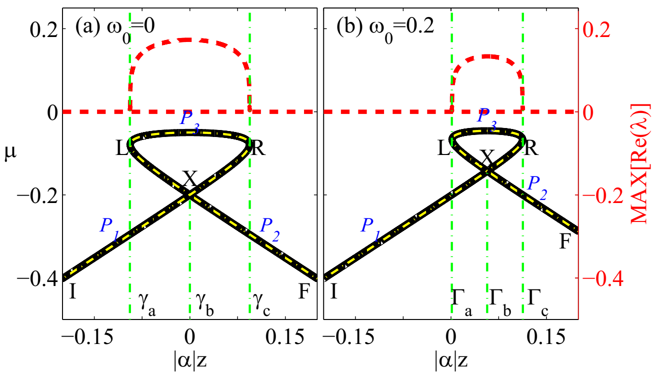

FIG. 3. Adiabatic energy levels and fixed-point stability analysis of ENTL for $v_0 = 0.2$. The dashed (red) lines represent the maximum real part of the eigenvalues of the Hamilton-Jacobi matrix. The solid (black) and dashed-dotted (yellow) lines represent the adiabatic energy levels corresponding to the forward and reverse sweep. Here, for the forward sweep, the nonlinear coefficient c takes 0.4; for the reverse sweep, the nonlinear coefficient takes $\frac{1-2\omega_0}{1+2\omega_0}c$. Furthermore, the eigenstates correspond to fixed points P_i ($i = 1, 2, 3$) in the classical Hamiltonian system H_c, whose trajectories are $P_1 \to IXR$, $P_2 \to LXF$, and $P_3 \to LR$.

We plot two sets of nonlinear adiabatic energy levels with different ω_0 in Fig. 3. We can see that a loop structure appears in both, which means that at the adiabatic limit $\alpha \to 0$, the nonlinear LZSM tunneling probability is nonzero, consistent with our direct simulation results. To reveal this interesting phenomenon, we consider an equivalent classical Hamiltonian. We define $a' = |a'|e^{i\theta_a}$, $b' = |b'|e^{i\theta_b}$, and let $\theta = \theta_b - \theta_a$, $s = (v_0 + 2v_0\omega_0)(|b'|^2 - |a'|^2)$. s and θ are a pair of canonical variables in a classical Hamiltonian system satisfying $\frac{ds}{dz} = -\frac{\partial H_c}{\partial \theta}$, $\frac{d\theta}{dz} = \frac{\partial H_c}{\partial s}$ [35]. A simple calculation gives the following classical Hamiltonian,

$$H_c = -\frac{1}{2}v_0 \cos\theta\sqrt{1-s^2}\sqrt{1-4\omega_0^2} + 2\gamma s + \frac{c(s^2 - 4\omega_0 s)}{2+4\omega_0}. \tag{18}$$

The above equation can be reduced to the standard model in Refs. [19,20] when $\omega_0 = 0$. The following equations give its fixed points,

$$\frac{\partial H_c}{\partial \theta} = \frac{1}{2}v_0 \sin\theta\sqrt{1-s^2}\sqrt{1-4\omega_0^2} = 0,$$
$$\frac{\partial H_c}{\partial s} = \frac{1}{2}\frac{v_0 s\cos\theta}{\sqrt{1-s^2}}\sqrt{1-4\omega_0^2} + 2\gamma + \frac{c(s-2\omega_0)}{1+2\omega_0} = 0. \tag{19}$$

The eigenstates of adiabatic energy levels correspond to fixed points. An unstable fixed point P_3 appears when a loop structure appears, as shown in Fig. 3. Therefore, we can judge the correctness of our adiabatic levels by analyzing the stability of fixed points. We get the following corresponding Hamilton-Jacobi matrix by linearizing Eq. (19) near the fixed points,

$$\begin{pmatrix} -\frac{\partial^2 H_c}{\partial\theta\partial s} & -\frac{\partial^2 H_c}{\partial\theta^2} \\ \frac{\partial^2 H_c}{\partial s^2} & \frac{\partial^2 H_c}{\partial s\partial\theta} \end{pmatrix}. \tag{20}$$

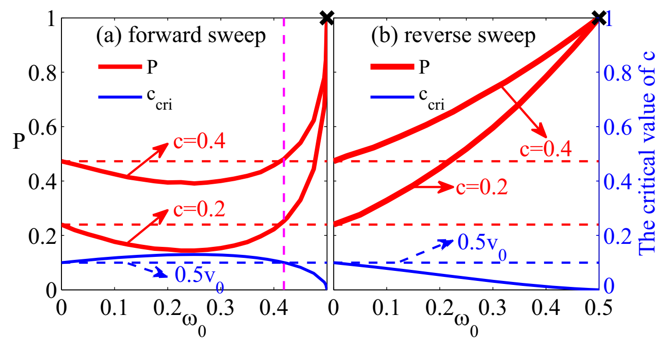

FIG. 4. Near-adiabatic tunneling probability and critical value of loop structure for $v_0 = 0.2$ and $\alpha = 0.0001$. The dashed lines are auxiliary lines for observing threshold values. The black cross indicates that the value at $\omega_0 = 0.5$ is not feasible, i.e., here, the model is invalid.

The fixed point is stable when the real part of the matrix's eigenvalue (λ) is zero. On the contrary, it is unstable. In Fig. 3, we verify the correctness of our nonlinear adiabatic energy levels. Reference [36] shows that the pair of canonical variables (θ, s) corresponding to the unstable fixed point P_3 at the adiabatic level crossing point X is $(\pi, 0)$. Then, by substituting $(\theta, s) = (\pi, 0)$ into Eq. (18), we get that the γ value corresponding to the point X is $c\omega_0/(1+2\omega_0)$, that is, the value corresponding to γ_b and Γ_b in Fig. 3. When P_i ($i = 1, 2, 3$) coincide at this moment, the loop structure is in a critical state, and the adiabatic tunneling probability is zero, i.e., the s values corresponding to the three points are -1, 1, and 0, respectively. In this case, we can get the critical value of the nonlinear coefficient to be $c_{\text{cri}} = \frac{v_0}{2}(1+2\omega_0)\sqrt{1-4\omega_0^2}$. When $v_0 = 2c_{\text{cri}}$, ω_0 is a threshold, below which the gain-dissipation term is inhibitory in adiabatic tunneling. On the contrary, it promotes it. Figure 4(a) proves this conclusion.

III. NONRECIPROCAL TUNNELING

In this section, we consider the case of the reverse sweep. Previous studies have found that the classical Hamiltonian is closely related to the tunneling probability. Therefore, we solve the equivalent classical Hamiltonian corresponding to ENTL in reverse sweep and compare it with forward sweep. First, we set the initial state to $(a, b) = (0, 1)$, thus the corresponding initial state in ENTL should be $(a', b') = [0, (v_0 - 2v_0\omega_0)^{-1/2}]$. In this case, the total population density is $N = \frac{1+2\omega_0}{1-2\omega_0} - \frac{4\omega_0}{1-2\omega_0}P$, and here, P is the tunneling probability of reverse sweep, equal to the value of $|b|^2$ in the final state (see Fig. 5). We recalculate Eq. (14), where γ in the formula is changed to $-\gamma'$, i.e., $\gamma' = |\alpha|z = \gamma$. Consistent with Eq. (18), we let $\theta' = \theta_b - \theta_a$, $s' = (v_0 - 2v_0\omega_0)(|a'|^2 - |b'|^2)$, then obtain

$$H_c' = -\frac{v_0}{2}\cos\theta'\sqrt{1-s'^2}\sqrt{1-4\omega_0^2} + 2\gamma' s' + \frac{c'(s'^2 - 4\omega_0 s')}{2+4\omega_0}. \tag{21}$$

Here, $c' = \frac{1+2\omega_0}{1-2\omega_0}c$. Compared with Eq. (18), we can see that the difference between forward and reverse sweep is

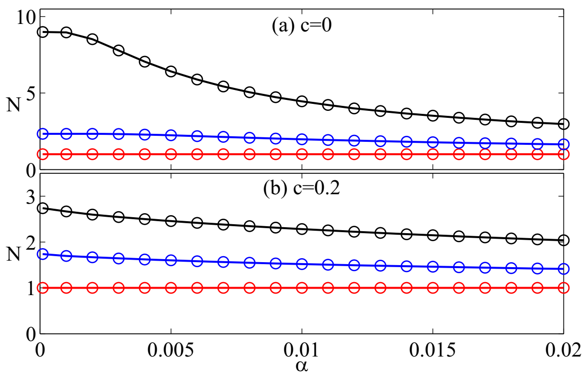

FIG. 5. The final total population density N under reverse sweep for $v_0 = 0.2$. From bottom to top, $\omega_0 = 0$, 0.2, and 0.4, respectively. Solid lines correspond to the NTL simulation results, and circular marks correspond to $N = \frac{1+2\omega_0}{1-2\omega_0} - \frac{4\omega_0}{1+2\omega_0}P$. Here, P is the tunneling probability under the reverse sweep (see Fig. 6).

only on the equivalent nonlinear coefficient. When ω_0 is not zero, the c' of the reverse sweep is greater than the corresponding c of the forward. Therefore, the adiabatic tunneling probability of the reverse sweep is greater than that of the forward. Moreover, the greater ω_0, the greater is the difference between the two. This is because the existence of ω_0 breaks the spatial inversion symmetry of the Hamiltonian and leads to the generation of nonreciprocal tunneling, consistent with the conclusions in Ref. [37]. We proved this conclusion through numerical simulation, as shown in Fig. 6. When we set the original nonlinear coefficient of reverse sweep as $\frac{1-2\omega_0}{1+2\omega_0}c_f$, where c_f is the nonlinear coefficient of forward sweep, the two classical Hamiltonians are completely consistent, and their tunneling probabilities should also be consistent, as shown in Fig. 6(e). Moreover, the threshold of the gain-dissipation term corresponding to the reverse sweep is obtained by $v_0 = \frac{1-2\omega_0}{1+2\omega_0}2c_{\text{cri}}$. In this case, when $\omega_0 > 0$, this term always plays a promoting role [see Fig. 4(b)].

We also study the quartic equation for the adiabatic energy level in the reverse sweep, which differs from Eqs. (16) and (17) only by $\omega_0 \to -\omega_0$. We plot two sets of adiabatic energy levels under reverse sweep in Fig. 3 with the yellow dashed-dotted lines, where the nonlinear coefficient we take is $\frac{1-2\omega_0}{1+2\omega_0}c_f$. According to Fig. 3, under such a nonlinear coefficient selection for the reverse sweep, the adiabatic energy level of the reverse sweep is the same as that of the forward sweep.

IV. CONCLUSION

We have studied the nonlinear LZSM problem in a class of non-Hermitian NTL systems. We have proposed a method for constructing ENTL and verified that the tunneling probabilities obtained by these two models are consistent. According to the equivalent form, we have given the expression of the total population density N, which shows that due to the effect of dissipation, N is no longer conserved, and will decay to a fixed value, which is related to the gain-dissipation coefficient ω_0 and the sweep velocity. By analyzing the equivalent classical Hamiltonian of ENTL, we have obtained a threshold value of ω_0, determined only by v_0. In the forward sweep, the adiabatic tunneling is inhibited below the threshold and promoted above it. The reverse sweep for $\omega_0 > 0$ is always promoted. Furthermore, we have found that systems with gain-dissipation terms are more sensitive to external drives. Finally, we have compared the classical Hamiltonians corresponding to the forward and reverse sweeps, proved the nonreciprocal tunneling caused by the spatial inversion symmetry breaking of the Hamiltonian, and verified it by numerical simulation.

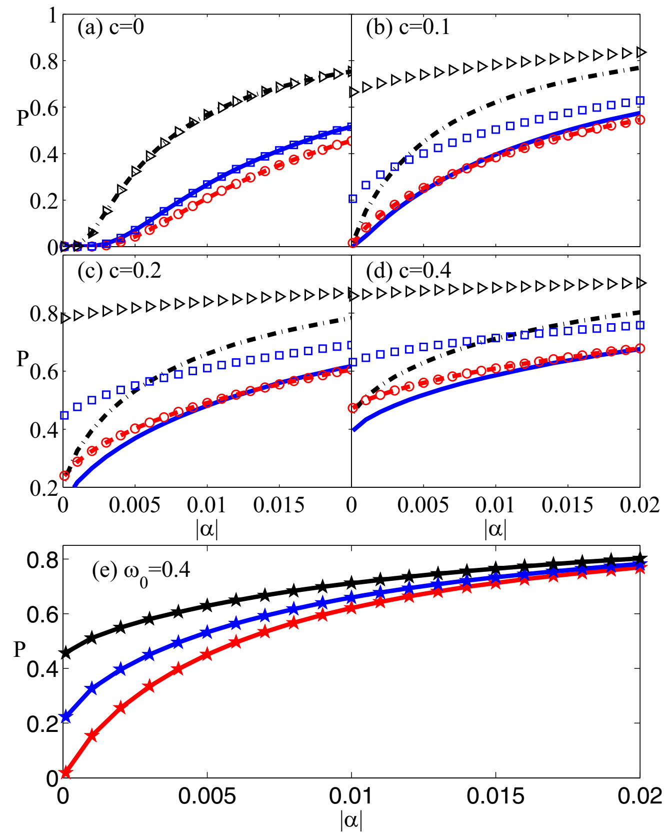

FIG. 6. Tunneling probability P for $v_0 = 0.2$ under forward and reverse sweeps. (a)–(d) The red circles, blue squares, and black triangles correspond to tunneling probabilities of $\omega_0 = 0$, 0.2, and 0.4 under reverse sweep, respectively. The red dashed, blue solid, and black dashed-dotted lines indicate the tunneling probabilities under forward sweep corresponding to $\omega_0 = 0$, 0.2, and 0.4. (e) The solid lines and star marks correspond to the tunneling probabilities of forward and reverse sweeps, respectively. From bottom to top, the nonlinear coefficients take $c = 0.1$, 0.2, and 0.4 for the forward sweep, and the corresponding nonlinear coefficients are $\frac{1-2\omega_0}{1+2\omega_0}c$ for the reverse sweep.

ACKNOWLEDGMENT

This work is supported by the Science and Technology Project of Hebei Education Department, China (Grant No. ZD2020200).

[1] C. M. Bender and S. Boettcher, Real spectra in non-Hermitian Hamiltonians having $\mathscr{PT}$ symmetry, Phys. Rev. Lett. **80**, 5243 (1998).

[2] V. V. Konotop, J. Yang, and D. A. Zezyulin, Nonlinear waves in $\mathcal{PT}$-symmetric systems, Rev. Mod. Phys. **88**, 035002 (2016).

[3] A. Lupu, H. Benisty, and A. Degiron, Switching using PT symmetry in plasmonic systems: Positive role of the losses, Opt. Express **21**, 21651 (2013).

[4] H. Benisty, A. Degiron, A. Lupu, A. D. Lustrac, S. Chénais, S. Forget, M. Besbes, G. Barbillon, A. Bruyant, S. Blaize, and G. Lérondel, Implementation of PT symmetric devices using plasmonics: Principle and applications, Opt. Express **19**, 18004 (2011).

[5] E. M. Graefe, H. J. Korsch, and A. E. Niederle, Mean-field dynamics of a non-Hermitian Bose-Hubbard dimer, Phys. Rev. Lett. **101**, 150408 (2008).

[6] W. Liu, M. Li, R. S. Guzzon, E. J. Norberg, J. S. Parker, M. Lu, L. A. Coldren, and J. Yao, An integrated parity-time symmetric wavelength-tunable single-mode microring laser, Nat. Commun. **8**, 15389 (2017).

[7] G. Arwas, S. Gadasi, I. Gershenzon, A. Friesem, N. Davidson, and O. Raz, Anyonic-parity-time symmetry in complex-coupled lasers, Sci. Adv. **8**, eabm7454 (2022).

[8] Y. Zhang, Z. Chen, B. Wu, T. Busch, and V. V. Konotop, Asymmetric loop spectra and unbroken phase protection due to nonlinearities in $\mathcal{PT}$-symmetric periodic potentials, Phys. Rev. Lett. **127**, 034101 (2021).

[9] L. D. Landau, Zur theorie der energieubertragung II, Z. Sowjetunion **2**, 46 (1932).

[10] C. Zener, Non-adiabatic crossing of energy levels, Proc. R. Soc. London A **137**, 696 (1932).

[11] E. C. G. Stückelberg, Theory of inelastic collisions between atoms, Helv. Phys. Acta (Basel) **5**, 369 (1932).

[12] E. Majorana, Atomi orientati in campo magnetico variabile, Nuovo Cim. **9**, 43 (1932).

[13] O. V. Ivakhnenko, S. N. Shevchenko, and F. Nori, Nonadiabatic Landau–Zener–Stückelberg–Majorana transitions, dynamics, and interference, Phys. Rep. **995**, 1 (2023).

[14] C. Ottaviani, V. Ahufinger, R. Corbalán, and J. Mompart, Adiabatic splitting, transport, and self-trapping of a Bose-Einstein condensate in a double-well potential, Phys. Rev. A **81**, 043621 (2010).

[15] Y.-A. Chen, S. D. Huber, S. Trotzky, I. Bloch, and E. Altman, Many-body Landau–Zener dynamics in coupled one-dimensional Bose liquids, Nat. Phys. **7**, 61 (2011).

[16] T. Morimoto and N. Nagaosa, Nonreciprocal current from electron interactions in noncentrosymmetric crystals: Roles of time reversal symmetry and dissipation, Sci. Rep. **8**, 2973 (2018).

[17] M. Wubs, K. Saito, S. Kohler, P. Hänggi, and Y. Kayanuma, Gauging a quantum heat bath with dissipative Landau-Zener transitions, Phys. Rev. Lett. **97**, 200404 (2006).

[18] D. Diakonov, L. M. Jensen, C. J. Pethick, and H. Smith, Loop structure of the lowest Bloch band for a Bose-Einstein condensate, Phys. Rev. A **66**, 013604 (2002).

[19] B. Wu and Q. Niu, Nonlinear Landau-Zener tunneling, Phys. Rev. A **61**, 023402 (2000).

[20] J. Liu, L. Fu, B.-Y. Ou, S.-G. Chen, D.-I. Choi, B. Wu, and Q. Niu, Theory of nonlinear Landau-Zener tunneling, Phys. Rev. A **66**, 023404 (2002).

[21] S. Ashhab, O. A. Ilinskaya, and S. N. Shevchenko, Nonlinear Landau-Zener-Stückelberg-Majorana problem, Phys. Rev. A **106**, 062613 (2022).

[22] M. Jona-Lasinio, O. Morsch, M. Cristiani, N. Malossi, J. H. Müller, E. Courtade, M. Anderlini, and E. Arimondo, Asymmetric Landau-Zener tunneling in a periodic potential, Phys. Rev. Lett. **91**, 230406 (2003).

[23] S. Matityahu, H. Schmidt, A. Bilmes, A. Shnirman, G. Weiss, A. V. Ustinov, M. Schechter, and J. Lisenfeld, Dynamical decoupling of quantum two-level systems by coherent multiple Landau–Zener transitions, NPJ Quantum Inf. **5**, 114 (2019).

[24] Q. Guan, M. K. H. Ome, T. M. Bersano, S. Mossman, P. Engels, and D. Blume, Nonexponential tunneling due to mean-field-induced swallowtails, Phys. Rev. Lett. **125**, 213401 (2020).

[25] A. Dey, D. Cohen, and A. Vardi, Adiabatic passage through chaos, Phys. Rev. Lett. **121**, 250405 (2018).

[26] X. Wang, H. D. Liu, and L. B. Fu, Nonlinear non-Hermitian Landau–Zener–Stückelberg–Majorana interferometry, New J. Phys. **25**, 043032 (2023).

[27] X. Shen, F. Wang, Z. Li, and Z. Wu, Landau-Zener-Stückelberg interferometry in $\mathcal{PT}$-symmetric non-Hermitian models, Phys. Rev. A **100**, 062514 (2019).

[28] W.-Y. Wang, B. Sun, and J. Liu, Adiabaticity in nonreciprocal Landau-Zener tunneling, Phys. Rev. A **106**, 063708 (2022).

[29] Z. H. Musslimani, K. G. Makris, R. El-Ganainy, and D. N. Christodoulides, Optical solitons in $\mathcal{PT}$ periodic potentials, Phys. Rev. Lett. **100**, 030402 (2008).

[30] X. Xu, Z. Zhang, and Z. Liang, Nonequilibrium Landau-Zener tunneling in exciton-polariton condensates, Phys. Rev. A **102**, 033317 (2020).

[31] B. Wu and Q. Niu, Superfluidity of Bose–Einstein condensate in an optical lattice: Landau–Zener tunnelling and dynamical instability, New J. Phys. **5**, 104 (2003).

[32] J. Yang and T. I. Lakoba, Universally-convergent squared-operator iteration methods for solitary waves in general nonlinear wave equations, Stud. Appl. Math. **118**, 153 (2007).

[33] S. Yu, S. Zhao, and G. W. Wei, Local spectral time splitting method for first- and second-order partial differential equations, J. Comput. Phys. **206**, 727 (2005).

[34] Y. Ekşioğlu, O. E. Müstecaplıoğlu, and K. Güven, Dissipative Josephson junction of an optical soliton and a surface plasmon, Phys. Rev. A **87**, 023823 (2013).

[35] J. Liu, B. Wu, and Q. Niu, Nonlinear evolution of quantum states in the adiabatic regime, Phys. Rev. Lett. **90**, 170404 (2003).

[36] Y. Cao and T. F. Xu, Nonlinear Landau-Zener tunneling under higher-order dispersion, Phys. Rev. A **107**, 032420 (2023).

[37] S. Kitamura, N. Nagaosa, and T. Morimoto, Nonreciprocal Landau–Zener tunneling, Commun. Phys. **3**, 63 (2020).